Forward-Kinematics-Based Approaches for Pose Accuracy of Docking Mechanism with Joint Clearance

Li Jianguang(李建广)[1*], *Ding Jian*(丁建)[1], *Yao Yingxue*(姚英学)[1],
Xu Chuntian(许春田)[1,2], *Jing Huaijing*(荆怀靖)[3],
Fang Honggen (方红根)[3], *Cao gang* (曹刚)[4]

1. School of Mechatronics Engineering, Harbin Institute of Technology, Harbin 150001, P. R. China;
2. School of Mechanical Engineering and Automation, University of Science and Technology, Liaoning Anshan 114051, P. R. China;
3. Shanghai Aerospace Equipments Manufacturer, Shanghai 200245, P. R. China;
4. State Grid Harbin Power Supply Company, Harbin 150090, P. R. China

(Received 19 May 2014; revised 17 November 2014; accepted 25 November 2014))

Abstract: Joint clearance, as an important stochastic factor, can significantly deteriorate positioning and repeatability accuracies and lower assembly quality of a 6-DOF docking mechanism. Considering pose accuracy with traditional error model that possesses inherent imprecision, both probabilistic and deterministic approaches based on forward kinematics are presented to analyze comprehensive pose error (CPE) in simulation. Results indicate an identical trend emerges for each CPE with both approaches, and both CPEs perform opposite variations as the moving platform upgrades. The findings provide theoretical reference for refinement of assembly quality evaluation of this mechanism.

Key words: joint clearance; docking mechanism; probabilistic approach; deterministic approach; comprehensive pose error (CPE)

CLC number: TH164 **Document code**: A **Article ID**: 1005-1120(2015)04-0365-07

0 Introduction

Joint clearance as an important stochastic error poses a big impact on pose accuracy of a six degree of freedom (DOF) docking mechanism. During assembly process, comprehensive pose error (CPE) is adopted as a main index to evaluate assembly quality, therefore, it is necessary to investigate comprehensive pose accuracy influenced by joint clearance.

Early researchers tend to combine joint clearances with dimensional tolerance together in accuracy analysis and dimensional synthesis. However, clearance error is stochastic, which is intrinsicly different from other source errors. The manners of output errors may also be various, and the accuracy analysis results thus become imprecise.

Voglewede et al.[1] examined the unconstrained motion of many parallel kinematic mechanism (PKM) with revolute or spherical passive joints due to clearances in those joints. They found unconstrained motion of end effectors by modeling the clearances, creating equivalent clearance manipulator, and utilizing standard workspace generation techniques on the virtual manipulator. Venanzi et al.[2] presented a model based on the displacement of each joint to express the pose errors of the end effecter as a function of geometrical parameters of the mechanism system. They[3] also adopted the principle of virtual works to assess the influence. A genetic model for kinematics pair is utilized, which can be applied to any other mechanism with an arbitrary

* **Corresponding author**: Li Jianguang, Professor, E-mail: mejgli@hit.edu.cn.

How to cite this article: Li Jianguang, Ding Jian, Yao Yingxue, et al. Forward-kinematics-based approaches for pose accuracy of docking mechanism with joint clearance[J]. Trans. Nanjing U. Aero. Astro., 2015,32(4):365-371.
http://dx.doi.org/10.16356/j.1005-1120.2015.04.365

number of links loaded by any kind of actions. Chebbi et al.[4] developed an analytical model to predict the pose error with static analysis of a 3-universal prismatic universal (3-UPU) parallel robot, and gave the distribution of the pose errors over the workspace of the robot. Wang et al.[5] presented a novel method based on trajectory planning to avoid the detachment of joint elements of a manipulator with clearances, and proposed an improved detachment criterion for the revolute and spherical joints. They obtained the dynamic response spectrums of joint forces, which can be used to facilitate such selection of the adjustable trajectory parameters as to avoid the detachment between joint elements. Zhu and Ting[6-7] brought forth a probability density function (PDF) for end pose of a robot based on statistical method. PDF is derived from joint deviation with specific distribution pattern, including normal and uniform. They also investigated the worst positioning error due to joint clearance in a single loop linkage, and obtained the maximum error when all the clearance links were collinear by modeling the joint clearance as a small link. Tsai et al.[8] treated joint clearance as a virtual link with no mass, analyzed the kinematics sensitivity of the mechanism with clearances using the screw theory, and finally solved mechanism positions based on both loop closure and reciprocal equations. They[9] subsequently utilized the screw theory to conduct accuracy analysis of a multi-loop linkage with joint clearance. Huang et al.[10] investigated the influence of joint clearance on positioning accuracy of a 2-DOF parallel robot, by assuming clearance distributions to be normally distributed and utilizing redundant constraints to reduce harmful clearance-due effects. Innocenti et al.[11] treated the spatial mechanism as a structure to assess clearance influence with the principle of virtual work.

Traditional pose error model based approach has long been accepted as a general form as $\delta x = \boldsymbol{J}\delta \boldsymbol{d}$, wherein δx represents the output errors; $\delta \boldsymbol{d}$ involves structural tolerance, joint clearances and other stochastic errors; $\boldsymbol{J}$ is regarded as a constant map matrix that corresponds to selected pose configuration. However, as infinitesimal displacement of PKM occurs due to joint clearance, the matrix $\boldsymbol{J}$ could no longer be kept constant but with a perturbation. In this sense, the pose error model becomes unreliable to some extent. The forward kinematics avoids map matrix $\boldsymbol{J}$ evaluation. It makes use of numerical method with arbitrary precision and the computational result is more reliable than that of the general pose error model with a closed form[12-15].

Here, the equivalent model of docking mechanism is established considering joint clearance. And the forward kinematics process is briefly introduced. On the basis of it, the probabilistic and deterministic approaches are detailed. Moreover, CPEs with both approaches are processed, and results are discussed.

1 Forward Kinematics Approach

1.1 Equivalent model

Fig. 1 (a) is a main structure of a 6-DOF docking mechanism composed of a Stewart platform and a set of translational chain system. The pose (x, y, z, α, β, γ) of the upper moving platform is controlled by six screw links driven by the lower translational chain involving a series of gear pairs and motors. Due to 12 joint clearances and source error accumulation from translational chain system, the pose errors of the upper moving platform may be out of the prescribed accuracy. How to effectively control these unstable error factors is an important issue.

At a given pose configuration, the manipulator becomes a structure but a mechanism as six links has been locked. Assuming that the pairs are in constant contact, a joint clearance can be modeled as a mass less virtual link with the length being one half of the joint clearance. Therefore, the structure could be transformed into a redundant mechanism as shown in Fig. 1(b). Furthermore, the equivalent simplification can be extended to other various 6-DOF parallel mechanisms with universal joint. Each leg can be modeled as a spherical joint, and clearance-due unconstrained motion of the platform can be treated as

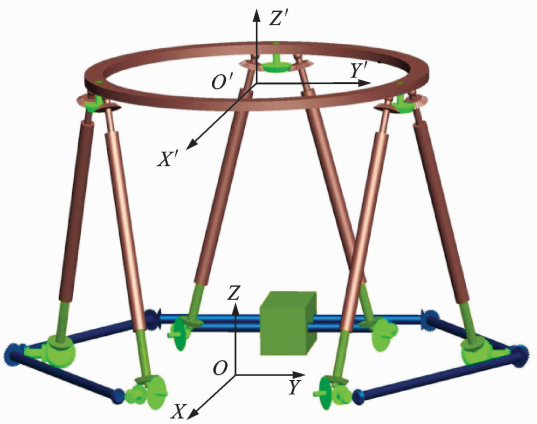

(a) Mechanical architecture

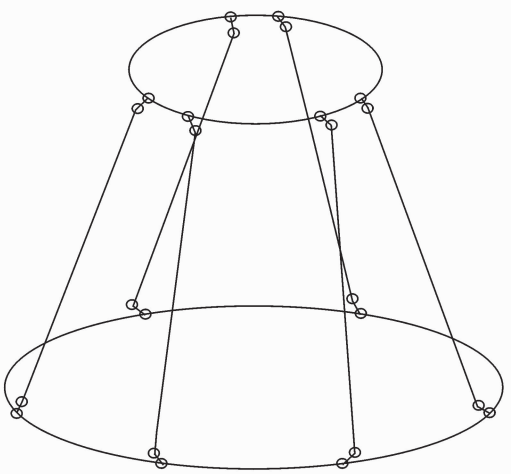

(b) Equivalent model

Fig. 1 6-DOF docking mechanism

equivalent as the Gough-Stewart platform(6-SPS) model [1].

1.2 Forward kinematics process

In general, forward kinematics is a process solving pose of mechanism given the lengths of 6 links. Newton-Raphson iteration method as one of effective numerical methods has been widely accepted in engineering computation for higher precision. The principle is expressed as follows[16-17]:

(1) Define objective function $\boldsymbol{f}$, where the components of $\boldsymbol{f}$ are the subtraction of actual link lengths and estimated ones.

(2) Choose the initial pose $\boldsymbol{P}$, which is not far from objective pose by estimation, and measure the lengths of 6 links.

(3) Calculate the length l_i ($i=1, 2, \cdots, 6$) via the parameter $\boldsymbol{P}$ using inverse kinematics.

(4) Check the norm of $\boldsymbol{P}$ as a termination condition. If $\boldsymbol{P}^{\mathrm{T}}\boldsymbol{P}<\varepsilon$, $\boldsymbol{P}$ is the identified pose solution and terminate, otherwise continue with step (5).

(5) Calculate the Jacobean matrix $\boldsymbol{J}=\partial \boldsymbol{f}/\partial \boldsymbol{P}$.

(6) Compute the estimation $\delta \boldsymbol{P}$ with $\boldsymbol{J}\delta \boldsymbol{P}=-\boldsymbol{f}$.

(7) If $\delta \boldsymbol{P}^{\mathrm{T}}\delta \boldsymbol{P}<\varepsilon$, terminate the programme and $\boldsymbol{P}$ is the identified pose solution, otherwise continue with step (8).

(8) Update the estimated $\boldsymbol{P}$ by $\boldsymbol{P}=\boldsymbol{P}+\delta \boldsymbol{P}$, then turn to step (2).

1.3 Probabilistic approach

Taking the i-th link as an example as shown in Fig. 2, the nominal length of the i-th link O_1O_2 can be denoted as l_{i0}. The micro displacement makes the i-th link deviate from O_1O_2 to $A'B'$. According to continuous contact hypothesis for kinematic pairs, the link length $A'B'$ equals to l_{i0}. Meanwhile, the actual link length $O_1'O_2$ (denoted as l_{ia}) is different from l_{i0}. Considering dimensional scale proportion between the link length and joint clearance, the vector angle between $A'B'$ and $O_1'O_2$ can be viewed as zero. Hence, the actual link length l_{ia} can be expressed as

$$l_{ia}=l_{i0}+r\cos\theta_1+r\cos\theta_2 \tag{1}$$

where r denotes the joint clearance, θ_1 and θ_2 are the vector angles of $O_1'A'$ and $O_1'O_2$, O_2B' and $O_1'O_2$ in terms of continuous contact hypothesis, respectively. Clearance r is kept constant. θ_1 and θ_2 follow uniform distribution within $(0, \pi)$. The deduction above is expanded to the rest five

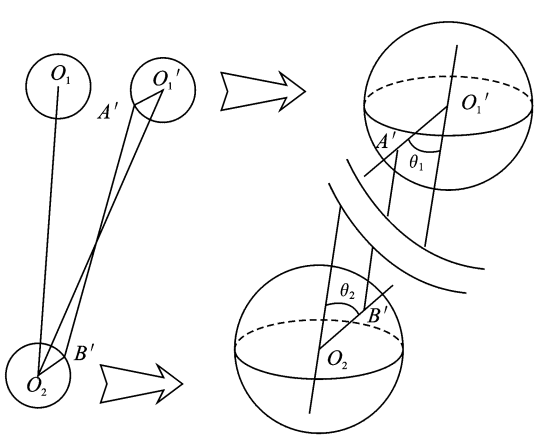

Fig. 2 Variation of actual link length

links. A sample set of actual links is put forward into a kinematics process, and a set of actual pose can be obtained. In addition, the pose errors can also be obtained through subtracting between the actual pose and the nominal one. The pose error distribution can be finally determined by investigating numerical characters of the pose error sample.

1.4 Deterministic approach

Each link of the mechanism serves as a two-force member when external force and wrench act on the moving platform, thus exhibiting the extinguish virtue of a parallel mechanism well-applied in engineering such as higher ratio of stiffness and mass. Actually, for a 6-DOF docking mechanism, each link has three states, i. e., extension, compression, and suspension. In this sense, a deterministic set of 6-force component can balance the moving platform whatever external force or wrench acts according to the equilibrium principle. In other words, the uncertainty input can be represented by a determined set of force combination. Thus, under the ideal circumstance, the center of the rod ball and the spherical shell of the joint are located at the same point. The ideal length of link is l_{i0}. While it is loaded, one considers that the ball joint structure is of three dimensions. For a single spherical joint, the rod ball will fall on the inner surface of the sphere shell with the principle of minimum potential energy due to action $\boldsymbol{F}$ from the link (Fig. 3). For both spherical joints, the centers of rod balls O_1, O_2 and the ones of shells O_3, O_4 will be geometrically in line with both contact points C_1, C_2, and the line coincides with the axis of the link. Therefore, the structure of a single chain with three dimensions can be reduced and illustrated by a problem with two dimensions.

(1) With the i-th link being extended, the actual length l_i is

$$l_i = l_{i0} + 2r \tag{2}$$

When the i-th link being compressed, the actual length l_i becomes

$$l_i = l_{i0} - 2r \tag{3}$$

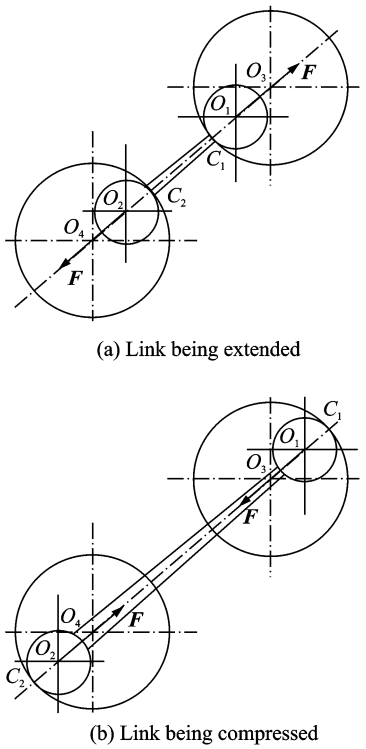

Fig. 3 Two states of the i-th link

(2) There is no action on the i-th link, thus being suspending. The actual length l_i can be expressed as

$$l_{i0} - 2r \leqslant l_i \leqslant l_{i0} + 2r \tag{4}$$

where r denotes the clearance of joints on the static and moving platforms.

There are 3^6 modes at a given pose configuration of 6-DOF docking mechanism. These modes can be classified into two categories: whether the link is suspended or not. (1) All the links are stressed, and the number of modes is 2^6; (2) Some links are suspending without any action on, and the number of modes is 3^6—2^6. However, according to the theory of interval analysis, these modes cannot form the worst case for pose errors. Therefore, only case (1) is considered. The actual link sets with 2^6 modes can cover all the extreme poses. Furthermore, pose error sequence can be obtained by subtraction with nominal pose.

2 Pose Errors Simulation

Examination is carried out to testify the assembly quality of docking mechanism at symmet-

ric pose configurations, in which only the pose parameter Z varies while the rest ones remain zero. The process is described as follows: the moving platform upgrades from the lowest point A to the highest point B in Fig. 4; A set of selected points by which the moving platform passes are examined for CPEs; Then the moving platform returns to A, and the points are examined once again. This process is repeated for several times. The assembly quality is evaluated by the obtained CPEs, which are defined as

$$\Delta r = \sqrt{\Delta x^2 + \Delta y^2} \tag{5}$$

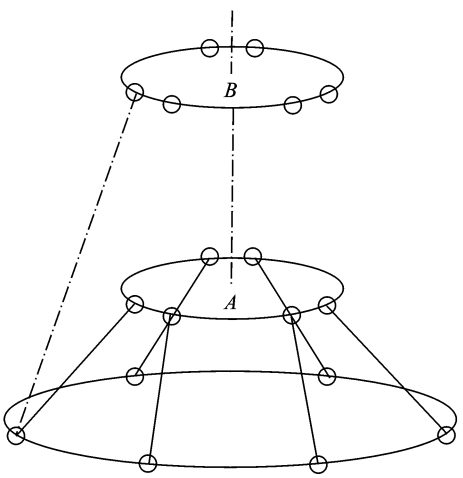

Fig. 4 Examination process for CPE

$$\Delta\theta = \sqrt{\Delta\alpha^2 + \Delta\beta^2} \tag{6}$$

where Δr is the comprehensive position error and $\Delta\theta$ the comprehensive orientation error. Δx and Δy are the position errors of the moving platform along X and Y axes, and $\Delta\alpha$ and $\Delta\beta$ the orientation errors of the platform along X and Y axes, respectively.

The examined points are selected at the height 500, 700, 900, 1 100, 1 300 and 1 500 mm of the moving platform. The structure parameters of the docking mechanism are listed in Tables 1, 2, where all of the joint clearances are 0.075 mm.

2.1 CPE with probabilistic approach

For each examined point between A and B in Fig. 4, the pose errors Δx, Δy, $\Delta\alpha$ and $\Delta\beta$ are processed with probabilistic approach discussed in Section 1.3 for a sample size of 10^5. The standard deviation of pose errors are obtained and listed in Table 3. Furthermore, to explore the relevance between Δx and Δy, $\Delta\alpha$ and $\Delta\beta$, the relevance coefficients ρ_{xy} and $\rho_{\alpha\beta}$ are introduced and listed in Table 3. They are defined as

$$\rho_{xy} = \frac{\mathrm{cov}(\Delta x, \Delta y)}{\sqrt{D(\Delta x)}\sqrt{D(\Delta y)}} \tag{7}$$

Table 1 Joint locations in coordination of moving platform

No.	1	2	3	4	5	6
x/mm	155.56	56.94	−212.50	−212.50	56.94	155.56
y/mm	155.56	212.50	56.94	−56.94	−212.50	−155.56

Table 2 Joint locations in coordination of base platform

No.	1	2	3	4	5	6
x/mm	531.26	−142.35	−388.91	−388.91	−142.35	531.26
y/mm	142.35	531.26	388.91	−388.91	−531.26	−142.35

Table 3 Standard deviations and covariances for pose errors

Height	500 mm	700 mm	900 mm	1 100 mm	1 300 mm	1 500 mm
$\sigma_{\Delta x}$/mm	0.098 6	0.124 9	0.153 4	0.183 3	0.213 0	0.243 3
$\sigma_{\Delta y}$/mm	0.098 6	0.125 2	0.153 5	0.182 5	0.213 5	0.244 4
$\sigma_{\Delta\alpha}$ /(°)	0.019 2	0.017 5	0.016 6	0.016 3	0.016 1	0.015 9
$\sigma_{\Delta\beta}$ /(°)	0.019 3	0.017 5	0.016 7	0.016 3	0.016 0	0.015 9
$\rho_{xy}/10^{-5}$	−1.29	0.257	10.4	8.31	4.29	14.7
$\rho_{\alpha\beta}/10^{-5}$	0.068	−0.005 5	0.14	0.023	0.038	0.12

$$\rho_{\alpha\beta} = \frac{\mathrm{cov}(\Delta\alpha, \Delta\beta)}{\sqrt{D(\Delta\alpha)}\sqrt{D(\Delta\beta)}} \tag{8}$$

where cov(•) represents the covariance of both stochastic variables, and $D(\bullet)$ the deviation of a stochastic variable. The means of Δx, Δy, $\Delta\alpha$ and $\Delta\beta$ approximate zeros as the pose configura-

tion is symmetric. They follow the Gaussian distribution: $\Delta x \sim N(0, \sigma_{\Delta x})$, $\Delta y \sim N(0, \sigma_{\Delta y})$, $\Delta\alpha \sim N(0, \sigma_{\Delta\alpha})$, $\Delta\beta \sim N(0, \sigma_{\Delta\beta})$ since each pose error is contributed by 12 stochastic clearances of joints[18]. Notice that in Table 3, $\sigma_{\Delta x}$ approaches $\sigma_{\Delta y}$, and $\sigma_{\Delta\alpha}$ approaches $\sigma_{\Delta\beta}$ for each point. There is little relevance between Δx and Δy because ρ_{xy} approximates zero. Similar results can be obtained from $\Delta\alpha$ and $\Delta\beta$, therefore, CPEs Δr and $\Delta\theta$ for six selected points follow the Rayleigh distributions with parameters $\sigma_{\Delta x}$ and $\sigma_{\Delta\alpha}$, respectively. Given a confidence level of 99.8%, CPEs Δr and $\Delta\theta$ are 3.525 times of the corresponding Rayleigh parameters, as listed in Table 4.

2.2 CPE with deterministic approach

For each point between A and B in Fig. 4, a sequence of pose errors Δx, Δy, $\Delta\alpha$ and $\Delta\beta$ with 2^6 combinations are obtained by deterministic approaches in Section 1.4, and the sequence of Δr and $\Delta\theta$ can also be obtained by the pose error sequence processed by Eqs. (5,6). The maximum ones in the sequence are singled out as Δr and $\Delta\theta$ of the point, as shown in Table 5.

Table 4 CPEs with probabilistic approach

Height	500 mm	700 mm	900 mm	1 100 mm	1 300 mm	1 500 mm
Δr /mm	0.347 6	0.440 3	0.540 7	0.646 1	0.750 8	0.857 6
$\Delta\theta$/(°)	0.067 7	0.061 7	0.058 5	0.057 5	0.056 8	0.056 0

Table 5 CPEs with deterministic approach

Height	500 mm	700 mm	900 mm	1 100 mm	1 300 mm	1 500 mm
Δr /mm	0.621 6	0.789 5	0.969 1	1.155	1.344 5	1.536 4
$\Delta\theta$/(°)	0.118 8	0.107 8	0.102 9	0.100 4	0.098 9	0.097 9

2.3 Contrast analysis

CPEs of examined points in Figs. 5,6 are illustrated with data in Tables 4,5. Firstly, Δr and $\Delta\theta$ in the deterministic approach are larger than those in the probabilistic approach, respectively. However, the trends of variations in both approaches are basically identical. The deterministic approach considers the worst case in 2^6 combinations for all the joint pairs, therefore, CPEs of each combination are limited in the estimated bounds. The probabilistic approach considers the deviation of joint clearance in view of statistical analysis. A reasonable scope of CPE is emphasized. As different evaluation methods for the particular error cannot be completely measured in practice, both deterministic and probabilistic approaches are important.

Secondly, Δr increases while $\Delta\theta$ decreases as the moving platform upgrades. Based on the opposite trend, reasonable points for examination can be sorted and the criterions for assembly quality evaluation can be further refined in terms of practical need for accuracy control and examination process.

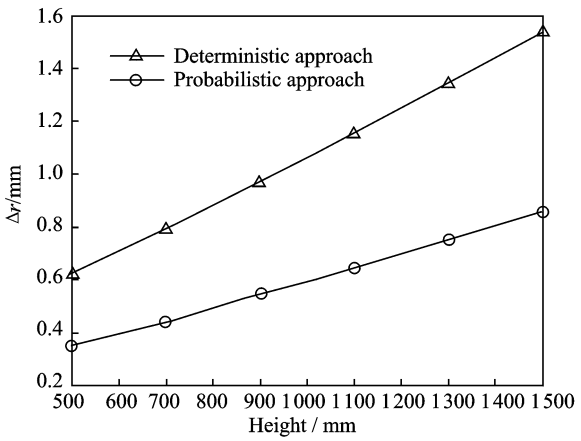

Fig. 5 Variation of Δr with increase of platform height

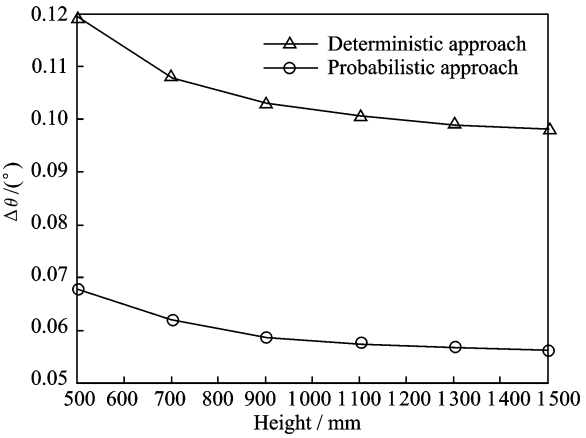

Fig. 6 Variation of $\Delta\theta$ with increase of platform height

3 Conclusions

Forward-kinematics-based approaches for comprehensive pose errors evaluations of 6-DOF docking mechanism are presented and discussed in detail with the consideration of joint clearance. Several conclusions are drawn as follows:

(1) A redundant 6-DOF docking mechanism model is established by considering joint clearance. The forward-kinematics-based probabilistic and deterministic approaches for pose errors are presented.

(2) Simulation results show that CPEs with the deterministic approach are larger than those with the probabilistic one. The variation trends of both approaches are basically identical. Thus, as different evaluations for a stochastic error, they are essential in assembly quality evaluation process for mechanism.

(3) CPEs exhibit opposite trends when the moving platform upgrades. It provides supplementay reference for further refinement of assembly quality evaluation.

Acknowledgements

This work was supported by the National Defense Basic Scientific Research Program (No. A0320110019) and the Shanghai Science and Technology Innovation Action Plan (No. 11DZ1120800).

References:

[1] Voglewede P, Uphoff I E. Application of workspace generation techniques to determine the unconstrained motion of PKMs [J]. Journal of Mechanical Design, 2004, 126:283-291.

[2] Venanzi S, Castelli V P. A new technique for clearance influence analysis in spatial mechanisms [J]. Journal of Mechanical Design, 2005, 127:446-455.

[3] Castelli V P, Venanzi S. Clearance influence analysis on mechanisms [J]. Mechanism and Machine Theory, 2005, 40(12): 1316-1329.

[4] Chebbi A H, Affi Z. Prediction of the pose errors produced by joints clearance for a 3-UPU parallel robot [J]. Mechanism and Machine Theory, 2009, 44(3):1768-1783.

[5] Wang H B, Liu Z Y. Detachment avoidance of joint elements of a robotic manipulator with clearances based on trajectory planning [J]. Mechanism and Machine Theory, 2010, 45(2):925-940.

[6] Zhu J, Ting K L. Uncertainty analysis of planar and spatial robots with joint clearances [J]. Mechanism and Machine Theory, 2000, 35(3):1239-1256.

[7] Ting K L, Zhu J M. The effects of joint clearance on position and orientation deviation of linkages and manipulators [J]. Mechanism and Machine Theory, 2000, 35(3): 391-401.

[8] Tsai M J, Lai T H. Kinematics sensitivity analysis of linkage with joint clearance based on transmission quality [J]. Mechanism and Machine Theory, 2004, 39(11): 1189-1206.

[9] Tsai M J, Lai T H. Accuracy analysis of a multi-loop linkage with joint clearances [J]. Mechanism and Machine Theory, 2008, 43(9):1141-1157.

[10] Huang T, Chetwynd D G. Tolerance design of a 2-DOF over constrained translational parallel robot [J]. IEEE Transactions on Robotics, 2006, 22(1): 167-172.

[11] Innocenti C. Kinematic clearance sensitivity analysis of spatial structures with revolute joints [J]. Journal of Mechanical Design, 2002, 124(1):52-57.

[12] Meng J, Zhang D J. Accuracy analysis of general PKMs with joint clearance[C]// IEEE International Conference on Robotics and Automation. Roma, Italy: IEEE, 2007:889-894.

[13] Meng J, Zhang D J. Accuracy analysis of PKMs with joint clearance [J]. Journal of Mechanical Design, 2009, 131:11-13.

[14] Biswas A, Derby S J. An iterative kinematic and force solution method for revolute joint with clearance [C]// Proceedings of the 1998 ASME Design Engineering Technical Conference. Atlanta, USA: [s. n.], 1998:156-162.

[15] Horie M, Funabashi H. A displacement analysis of spatial four-bar mechanisms [J]. Bulletin of JSME, 1985, 28:1535-1542.

[16] Wang J, Masory O. On the accuracy of a Stewart platform—Part I: The effect of manufacturing tolerances[C]//IEEE International Conference on Robotics and Automation. Atlanta, USA: IEEE, 1993:114-120.

[17] Yang X L, Wu H T, Chen B, et al. Fast numerical solution to forward kinematics of general Stewart mechanism using quaternion [J]. Trans Nanjing U Aero Astro, 2014, 31(4):377-385.

[18] Morris H D, Mark J S. Probability and statistics [M]. Beijing: China Machine Press, 2012:100-131.

(Executive editor: Zhang Tong)